

# Single-top production in the Standard Model and beyond

NIKOLAOS KIDONAKIS<sup>1</sup>

*Department of Physics*

*Kennesaw State University, Kennesaw, GA 30144, USA*

I present high-order calculations for single-top production in the Standard Model and in models with anomalous top-quark couplings. Theoretical results are presented for total cross sections and top-quark transverse momentum and rapidity distributions for the  $t$  and  $s$  single-top channels as well as for the associated production of a top quark with a  $W$  boson in the Standard Model. Corrections from soft-gluon emission through NNNLO are included. I also show results for the associated production of a top quark with a  $Z$  boson in processes involving anomalous top-quark couplings.

PRESENTED AT

CIPANP2018

Palm Springs, California, May 29–June 3, 2018

---

<sup>1</sup>This material is based upon work supported by the National Science Foundation under Grant No. PHY 1519606.

# 1 Higher-order soft-gluon corrections

It has been well known for some time that higher-order QCD corrections are significant in top-quark production processes. Fixed-order results for single-top production are known at NLO [1, 2] and some at NNLO [3, 4, 5, 6].

For single-top [7, 8, 9] (as well as top-antitop [9, 10]) processes at Tevatron and LHC energies, it is also well-known that soft-gluon corrections are important, and that they approximate exact results very well to the order in which the latter are known. Further higher-order soft-gluon corrections provide an additional theoretical improvement. Here I provide results with soft-gluon corrections for  $t$ -channel and  $s$ -channel single-top production, and  $tW$  production [7, 8, 9]. I also present results for  $tZ$  production via anomalous top-quark couplings [11].

For partonic processes of the form

$$f_1(p_1) + f_2(p_2) \rightarrow t(p_t) + X \quad (1)$$

we define  $s = (p_1 + p_2)^2$ ,  $t = (p_1 - p_t)^2$ ,  $u = (p_2 - p_t)^2$  and  $s_4 = s + t + u - \sum m^2$ . At partonic threshold  $s_4 \rightarrow 0$ . Soft-gluon corrections appear in the perturbative corrections as plus distributions involving logarithms of  $s_4$ , i.e.  $[\ln^k(s_4/m_t^2)/s_4]_+$ .

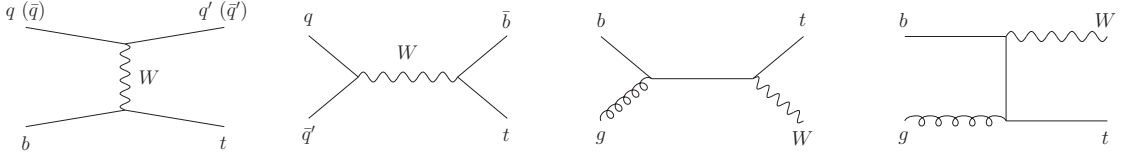


Figure 1: Lowest-order diagrams for single-top  $t$ -channel (left),  $s$ -channel (second from left), and  $tW$  (right two diagrams) production.

We resum these soft-gluon corrections for the double-differential cross section at NNLL accuracy, which requires the calculation of two-loop soft anomalous dimensions [7, 12, 13]. Taking moments of the partonic cross section with moment variable  $N$ ,  $\hat{\sigma}(N) = \int (ds_4/s) e^{-Ns_4/s} \hat{\sigma}(s_4)$ , we write a factorized expression for the cross section

$$\begin{aligned} \sigma^{f_1 f_2 \rightarrow tX}(N, \epsilon) &= H_{IL}^{f_1 f_2 \rightarrow tX}(\alpha_s(\mu_R)) S_{LI}^{f_1 f_2 \rightarrow tX}\left(\frac{m_t}{N\mu_F}, \alpha_s(\mu_R)\right) \\ &\times \prod J_{\text{in}}(N, \mu_F, \epsilon) \prod J_{\text{out}}(N, \mu_F, \epsilon) \end{aligned} \quad (2)$$

where  $H_{IL}^{f_1 f_2 \rightarrow tX}$  is a hard-scattering function and  $S_{LI}^{f_1 f_2 \rightarrow tX}$  is a soft-gluon function.

The evolution of the soft function, which gives the exponentiation of logarithms of  $N$ , follows from the renormalization group equation

$$\left(\mu \frac{\partial}{\partial \mu} + \beta(g_s) \frac{\partial}{\partial g_s}\right) S_{LI} = -(\Gamma_S^\dagger)_{LK} S_{KI} - S_{LK} (\Gamma_S)_{KI} \quad (3)$$

where  $\Gamma_S$  is the (process-dependent) soft anomalous dimension. The resummed cross section may be written as a product of exponentials, involving universal terms describing collinear and soft-gluon emission from incoming and outgoing partons, as well as process-specific terms that describe noncollinear soft-gluon emission and that depend explicitly on the process and its color structure.

We use the resummed cross section as a generator of finite-order expansions, and we provide approximate NNLO (aNNLO) and approximate N<sup>3</sup>LO (aN<sup>3</sup>LO) predictions for cross sections and differential distributions.

## 2 $t$ -channel production

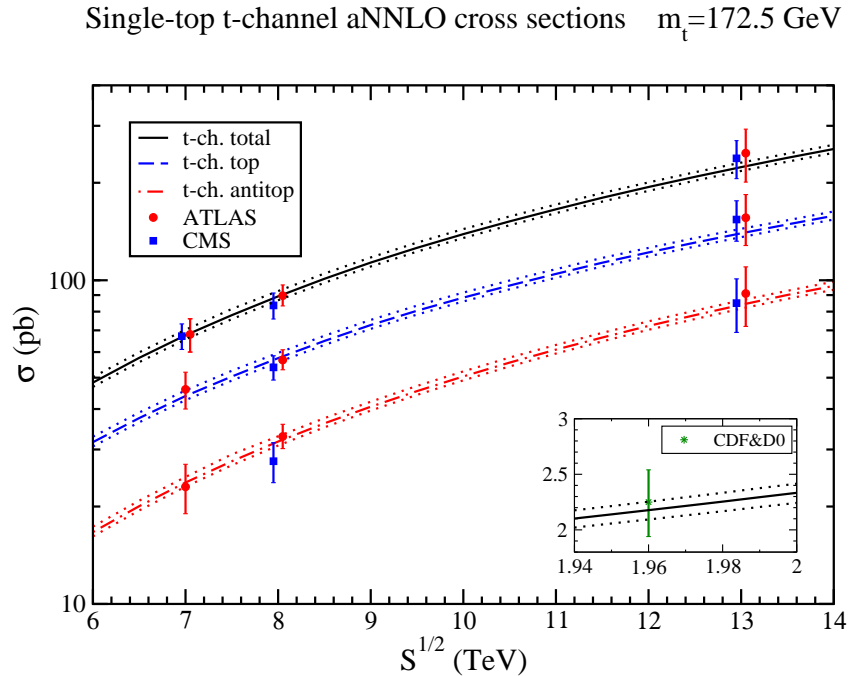


Figure 2: Single-top aNNLO  $t$ -channel cross sections compared with CMS and ATLAS data at 7 TeV [15, 16], 8 TeV [17, 18], and 13 TeV [19, 20], and (inset) with CDF and D0 combination data at 1.96 TeV [21].

We begin with single-top production in the  $t$ -channel. The leading-order diagram is shown in Fig. 1.

The soft anomalous dimension for this process is a  $2 \times 2$  matrix whose elements in a  $t$ -channel singlet-octet color basis at one loop in Feynman gauge are

$$\Gamma_{S11}^{t(1)} = C_F \left[ \ln \left( \frac{t(t - m_t^2)}{m_t s^{3/2}} \right) - \frac{1}{2} \right],$$

$$\begin{aligned}
\Gamma_{S12}^{t(1)} &= \frac{C_F}{2N} \ln \left( \frac{u(u - m_t^2)}{s(s - m_t^2)} \right), & \Gamma_{S21}^{t(1)} &= \ln \left( \frac{u(u - m_t^2)}{s(s - m_t^2)} \right), \\
\Gamma_{S22}^{t(1)} &= C_F \ln \left( \frac{s - m_t^2}{m_t \sqrt{s}} \right) - \frac{1}{2N} \ln \left( \frac{t(t - m_t^2)}{s(s - m_t^2)} \right) + \frac{(N^2 - 2)}{2N} \ln \left( \frac{u(u - m_t^2)}{s(s - m_t^2)} \right) - \frac{C_F}{2}.
\end{aligned} \tag{4}$$

At two loops, we only need the first matrix element:

$$\Gamma_{S11}^{t(2)} = \left[ C_A \left( \frac{67}{36} - \frac{\zeta_2}{2} \right) - \frac{5}{18} n_f \right] \Gamma_{S11}^{t(1)} + C_F C_A \frac{(1 - \zeta_3)}{4}. \tag{5}$$

We next provide numerical results for  $t$ -channel production at aNNLO. We use MMHT 2014 pdf [14]. Figure 2 shows the theoretical aNNLO  $t$ -channel production cross sections for single top, single antitop, and their sum, compared with data from the LHC and the Tevatron. Excellent agreement is observed between theory and data in all cases.

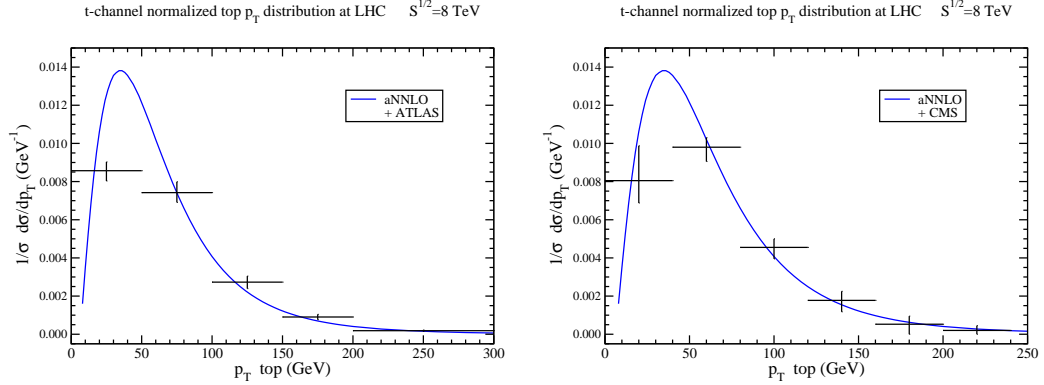


Figure 3: The aNNLO top-quark normalized  $p_T$  distributions in  $t$ -channel production at 8 TeV compared to (left) ATLAS [18] and (right) CMS [22] data.

The aNNLO top-quark normalized  $p_T$  distributions in  $t$ -channel production at 8 TeV energy are shown in Fig. 3 and compared with LHC data; we again note the very good description of the data by the theory curves.

### 3 $s$ -channel production

We continue with single-top production in the  $s$ -channel. The leading-order diagram is shown in Fig. 1.

Single-top  $s$ -channel aNNLO cross sections  $m_t=172.5$  GeV

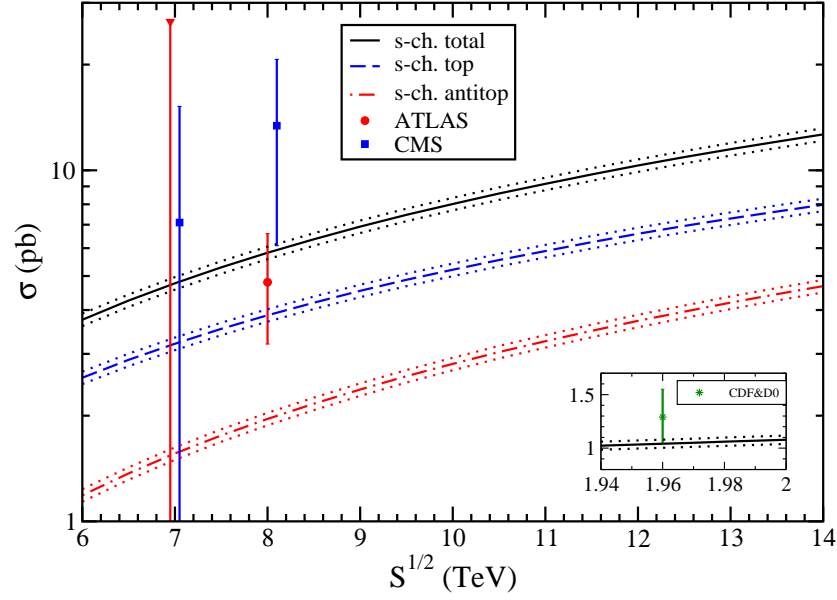


Figure 4: Single-top aNNLO  $s$ -channel cross sections compared to ATLAS and CMS data at 7 TeV [23, 24] and 8 TeV [24, 25], and (inset) to CDF and D0 combination data [26] at 1.96 TeV.

The soft anomalous dimension for this process is a  $2 \times 2$  matrix whose elements in an  $s$ -channel singlet-octet color basis at one loop in Feynman gauge are

$$\begin{aligned}
 \Gamma_{S11}^{s(1)} &= C_F \left[ \ln \left( \frac{s - m_t^2}{m_t \sqrt{s}} \right) - \frac{1}{2} \right], \\
 \Gamma_{S12}^{s(1)} &= \frac{C_F}{2N} \ln \left( \frac{u(u - m_t^2)}{t(t - m_t^2)} \right), \quad \Gamma_{S21}^{s(1)} = \ln \left( \frac{u(u - m_t^2)}{t(t - m_t^2)} \right), \\
 \Gamma_{S22}^{s(1)} &= C_F \ln \left( \frac{s - m_t^2}{m_t \sqrt{s}} \right) - \frac{1}{N} \ln \left( \frac{u(u - m_t^2)}{t(t - m_t^2)} \right) + \frac{N}{2} \ln \left( \frac{u(u - m_t^2)}{s(s - m_t^2)} \right) - \frac{C_F}{2}. \quad (6)
 \end{aligned}$$

At two loops, we only need the first matrix element:

$$\Gamma_{S11}^{s(2)} = \left[ C_A \left( \frac{67}{36} - \frac{\zeta_2}{2} \right) - \frac{5}{18} n_f \right] \Gamma_{S11}^{s(1)} + C_F C_A \frac{(1 - \zeta_3)}{4}. \quad (7)$$

Figure 4 shows the theoretical aNNLO  $s$ -channel production cross sections, using MMHT 2014 pdf [14], for single top, single antitop, and their sum, compared with available data from the LHC and the Tevatron.

## 4 Associated $tW$ production

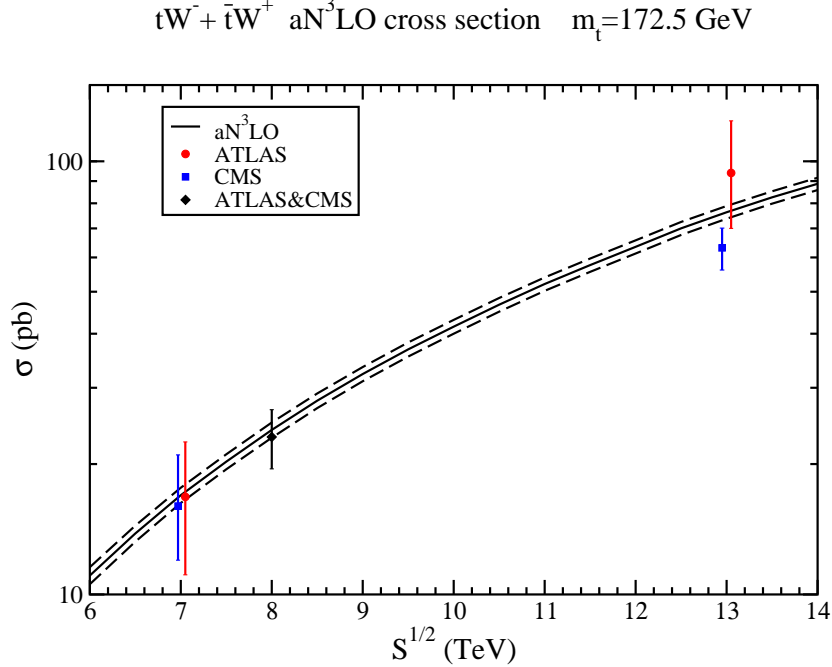


Figure 5: Single-top aN<sup>3</sup>LO cross sections for  $tW$  production compared to ATLAS and CMS data at 7 TeV [28, 29], 8 TeV [30], and 13 TeV [31, 32].

We continue with single-top production in association with a  $W$  boson. The leading-order diagrams for  $tW$  production are shown in Fig. 1.

The soft anomalous dimension for this process at one loop in Feynman gauge is

$$\Gamma_S^{tW^-(1)} = C_F \left[ \ln \left( \frac{m_t^2 - t}{m_t \sqrt{s}} \right) - \frac{1}{2} \right] + \frac{C_A}{2} \ln \left( \frac{m_t^2 - u}{m_t^2 - t} \right). \quad (8)$$

At two loops, we have

$$\Gamma_S^{tW^-(2)} = \left[ C_A \left( \frac{67}{36} - \frac{\zeta_2}{2} \right) - \frac{5}{18} n_f \right] \Gamma_S^{tW^-(1)} + C_F C_A \frac{(1 - \zeta_3)}{4}. \quad (9)$$

Figure 5 shows the theoretical aN<sup>3</sup>LO results for the sum of the  $tW^-$  and  $\bar{t}W^+$  cross sections, using MMHT 2014 pdf [14], compared with data from the LHC. Excellent agreement is found between theory and data for all LHC energies. The soft-gluon corrections are large; we note that large corrections are also found in related  $W$  and  $Z$  production processes at high  $p_T$  [27].

Figure 6 shows the aN<sup>3</sup>LO top-quark  $p_T$  and rapidity distributions in  $tW$  production. As the inset plot on the right shows, the aN<sup>3</sup>LO corrections are significant and increase at higher rapidities.

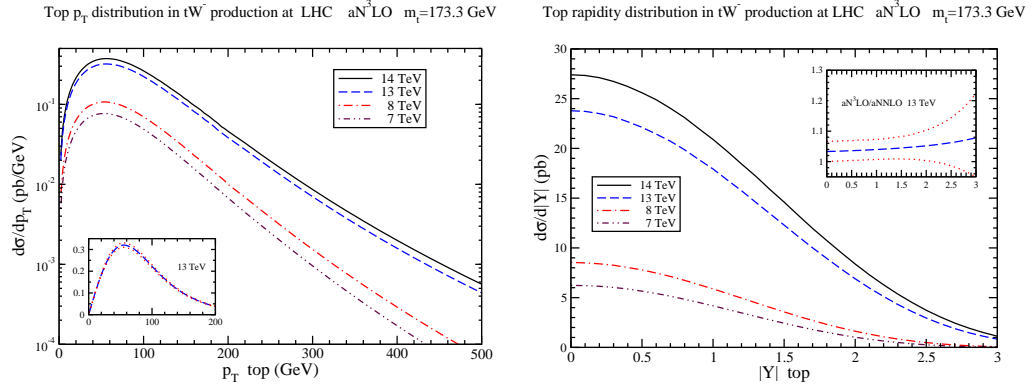


Figure 6: Top-quark aN<sup>3</sup>LO differential distributions in (left)  $p_T$  and (right) rapidity in  $tW^-$  production.

## 5 $tZ$ production via anomalous couplings



Figure 7: Lowest-order diagrams for  $tZ$  production via anomalous couplings.

In addition to Standard Model processes for top production, top quarks may also be produced via anomalous top-quark couplings [11, 33]. Here we study  $tZ$  production via such couplings [11]. A Lagrangian for such processes is given by

$$\Delta\mathcal{L}^{eff} = \frac{1}{\Lambda} \kappa_{tqZ} e \bar{t} (i/2) (\gamma_\mu \gamma_\nu - \gamma_\nu \gamma_\mu) q F_Z^{\mu\nu} + h.c. \quad (10)$$

Figure 7 shows the leading-order diagrams for the process  $gu \rightarrow tZ$ ; the similar process  $gc \rightarrow tZ$  also contributes.

The NLO corrections to these processes were calculated in Ref. [34], and we find that they are dominated by soft gluons. In our numerical results below we use CT14 [35] pdf.

In Fig. 8 we show aNNLO results for  $tZ$  production. The left plot shows total cross sections at LHC energies for  $gu \rightarrow tZ$  while the right plot shows the top-quark rapidity distributions for  $gc \rightarrow tZ$ . The insets in both plots show the aNNLO/NLO ratios, which demonstrate that the higher-order soft-gluon corrections are large, especially at large rapidities.

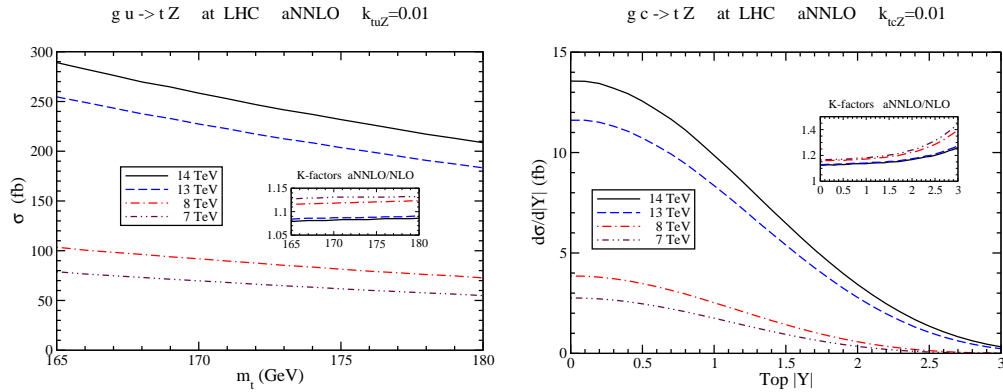


Figure 8: (Left) Total cross sections at aNNLO [11] for  $tZ$  production via  $gu \rightarrow tZ$ ; (Right) Top-quark rapidity distributions at aNNLO for  $tZ$  production via  $gc \rightarrow tZ$ .

These theoretical results may be useful in setting limits on the couplings, which is an area of active study by the LHC experiments [36, 37].

## 6 Summary

I have presented cross sections and differential distributions for single-top production. Results with soft-gluon corrections at aNNLO for  $t$ -channel and  $s$ -channel production, and at aN<sup>3</sup>LO for  $tW$  production, have been presented for total cross sections and top-quark  $p_T$  and rapidity distributions. The soft-gluon corrections are significant and we find excellent agreement of the theory with LHC and Tevatron data.

I have also presented aNNLO results for  $tZ$  production via anomalous top-quark couplings. Soft-gluon corrections are also very significant for this process.

## References

- [1] B.W. Harris, E. Laenen, L. Phaf, Z. Sullivan, and S. Weinzierl, Phys. Rev. D **66**, 054024 (2002) [hep-ph/0207055].
- [2] S.H. Zhu, Phys. Lett. B **524**, 283 (2002) [Erratum: *ibid.* **537**, 351 (2002)] [hep-ph/0109269].
- [3] M. Brucherseifer, F. Caola, and K. Melnikov, Phys. Lett. B **736**, 58 (2014) [arXiv:1404.7116 [hep-ph]].
- [4] E.L. Berger, J. Gao, C.-P. Yuan, and H.X. Zhu, Phys. Rev. D **94**, 071501 (2016) [arXiv:1606.08463 [hep-ph]].

- [5] E.L. Berger, J. Gao, and H.X. Zhu, JHEP **1711**, 158 (2017) [arXiv:1708.09405 [hep-ph]].
- [6] Z. Liu and J. Gao, arXiv:1807.03835 [hep-ph].
- [7] N. Kidonakis, Phys. Rev. D **81**, 054028 (2010) [arXiv:1001.5034 [hep-ph]]; **82**, 054018 (2010) [arXiv:1005.4451 [hep-ph]]; **83**, 091503(R) (2011) [arXiv:1103.2792 [hep-ph]]; **88**, 031504(R) (2013) [arXiv:1306.3592 [hep-ph]]; **93**, 054022 (2016) [arXiv:1510.06361 [hep-ph]].
- [8] N. Kidonakis, Phys. Rev. D **96**, 034014 (2017) [arXiv:1612.06426 [hep-ph]]; in Proceedings of DPF 2017, eConf C170731 [arXiv:1709.06975 [hep-ph]].
- [9] N. Kidonakis, in Physics of Heavy Quarks and Hadrons, HQ2013 [arXiv:1311.0283 [hep-ph]]; Int. J. Mod. Phys. A (in press) [arXiv:1806.03336 [hep-ph]].
- [10] N. Kidonakis, Phys. Rev. D **90**, 014006 (2014) [arXiv:1405.7046 [hep-ph]]; **91**, 031501(R) (2015) [arXiv:1411.2633 [hep-ph]]; **91**, 071502(R) (2015) [arXiv:1501.01581 [hep-ph]].
- [11] N. Kidonakis, Phys. Rev. D **97**, 034028 (2018) [arXiv:1712.01144 [hep-ph]].
- [12] N. Kidonakis, Phys. Rev. Lett. **102**, 232003 (2009) [arXiv:0903.2561 [hep-ph]].
- [13] N. Kidonakis, Int. J. Mod. Phys. A **31**, 1650076 (2016) [arXiv:1601.01666 [hep-ph]].
- [14] L.A. Harland-Lang, A.D. Martin, P. Molytinski, and R.S. Thorne, Eur. Phys. J. C **75**, 204 (2015) [arXiv:1412.3989 [hep-ph]].
- [15] CMS Collab., JHEP **1212**, 035 (2012) [arXiv:1209.4533 [hep-ex]].
- [16] ATLAS Collab., Phys. Rev. D **90**, 112006 (2014) [arXiv:1406.7844 [hep-ex]].
- [17] CMS Collab., JHEP **1406**, 090 (2014) [arXiv:1403.7366 [hep-ex]].
- [18] ATLAS Collab., Eur. Phys. J. C **77**, 531 (2017) [arXiv:1702.02859 [hep-ex]].
- [19] ATLAS Collab., JHEP **1704**, 086 (2017) [arXiv:1609.03920 [hep-ex]].
- [20] CMS Collab., Phys. Lett. B **772**, 752 (2017) [arXiv:1610.00678 [hep-ex]].
- [21] CDF and D0 Collab., Phys. Rev. Lett. **115**, 152003 (2015) [arXiv:1503.05027 [hep-ex]].
- [22] CMS Collab., CMS-PAS-TOP-14-004.

- [23] ATLAS Collab., ATLAS-CONF-2011-118.
- [24] CMS Collab., JHEP **1609**, 027 (2016) [arXiv:1603.02555 [hep-ex]].
- [25] ATLAS Collab., Phys. Lett. B **756**, 228 (2016) [arXiv:1511.05980 [hep-ex]].
- [26] CDF and D0 Collab., Phys. Rev. Lett. **112**, 231803 (2014) [arXiv:1402.5126 [hep-ex]].
- [27] N. Kidonakis and A. Sabio Vera, JHEP **0402**, 027 (2004) [hep-ph/0311266]; N. Kidonakis and R.J. Gonsalves, Phys. Rev. D **89**, 094022 (2014) [arXiv:1404.4302 [hep-ph]].
- [28] ATLAS Collab., Phys. Lett. B **716**, 142 (2012) [arXiv:1205.5764 [hep-ex]].
- [29] CMS Collab., Phys. Rev. Lett. **110**, 022003 (2013) [arXiv:1209.3489 [hep-ex]].
- [30] ATLAS and CMS Collab., ATLAS-CONF-2016-023, CMS-PAS-TOP-15-019.
- [31] ATLAS Collab., JHEP **1801**, 063 (2018) [arXiv:1612.07231 [hep-ex]].
- [32] CMS Collab., arXiv:1805.07399 [hep-ex].
- [33] A. Belyaev and N. Kidonakis, Phys. Rev. D **65**, 037501 (2002) [hep-ph/0102072]; N. Kidonakis and A. Belyaev, JHEP **0312**, 004 (2003) [hep-ph/0310299].
- [34] B.H. Li, Y. Zhang, C.S. Li, J. Gao, and H.X. Zhu, Phys. Rev. D **83**, 114049 (2011) [arXiv:1103.5122 [hep-ph]].
- [35] S. Dulat, T.-J. Hou, J. Gao, M. Guzzi, J. Huston, P. Nadolsky, J. Pumplin, C. Schmidt, D. Stump, and C.-P. Yuan, Phys. Rev. D **93**, 033006 (2016) [arXiv:1506.07443 [hep-ph]].
- [36] CMS Collaboration, JHEP **1707**, 003 (2017) [arXiv:1702.01404 [hep-ex]].
- [37] ATLAS Collaboration, ATLAS-CONF-2017-070.